International Journal of Nanomedicine

Dovepress
open access to scientific and medical research

Open Access Full Text Article

ORIGINAL RESEARCH

Topical Delivery of microRNA-125b by Framework Nucleic Acids for Psoriasis Treatment

Yunfeng Han[1], Long Xi[1,2], Fang Leng[3], Chenjie Xu[3], Ying Zheng[1]

[1]State Key Laboratory of Quality Research in Chinese Medicine, Institute of Chinese Medical Sciences, University of Macau, Macau, 999078, People's Republic of China; [2]School of Pharmaceutical Sciences, Guangzhou University of Chinese Medicine, Guangzhou, 510006, People's Republic of China; [3]Department of Biomedical Engineering, City University of Hong Kong, Hong Kong SAR, People's Republic of China

Correspondence: Ying Zheng; Chenjie Xu, Tel +853 88224687; +852 34424169, Fax +853 28841358, Email yzheng@umac.mo; chenjie.xu@cityu.edu.hk

Purpose: Psoriasis is a chronic and recurrent inflammatory dermatitis characterized by T cell imbalance and abnormal keratinocyte proliferation. MicroRNAs (miRNAs) hold promise as therapeutic agents for this disease; however, their clinical application is hindered by poor stability and limited skin penetration. This study demonstrates the utilization of Framework Nucleic Acid (FNA) for the topical delivery of miRNAs in psoriasis treatment.

Methods: By utilizing miRNA-125b as the model drug, FNA-miR-125b was synthesized via self-assembly. The successful synthesis and stability of FNA-miR-125b in bovine fetal serum (FBS) were verified through gel electrophoresis. Subsequently, flow cytometry was employed to investigate the cell internalization on HaCaT cells, while qPCR determined the effects of FNA-miR-125b on cellular functions. Additionally, the skin penetration ability of FNA-miR-125b was assessed. Finally, a topical administration study involving FNA-miR-125b cream on imiquimod (IMQ)-induced psoriasis mice was conducted to evaluate its therapeutic efficacy.

Results: The FNA-miR-125b exhibited excellent stability, efficient cellular internalization, and potent inhibition of keratinocyte proliferation. In the psoriasis mouse model, FNA-miR-125b effectively penetrated the skin tissue, resulting in reduced epidermal thickness and PASI score, as well as decreased levels of inflammatory cytokines.

Keywords: psoriasis, topical delivery, miRNA-125b, framework nucleic acid, FNA

Introduction

Psoriasis is a chronic and recurrent inflammatory dermatitis that manifests with both physical and physiological symptoms.[1] It primarily arises from an imbalance in T cell populations, as well as the abnormal proliferation and aberrant differentiation of keratinocytes.[1,2] Therefore, the treatment strategies of psoriasis focus on inhibit the T helper cell function or hyperplasia of keratinocyte. Existing therapies focus on temporarily relieving the symptoms using immunosuppressive drugs such as cyclosporine and methotrexate and monoclonal antibodies like TNF-α and IL-17 antibodies.[3] However, there is still no cure for psoriasis. There is a great need to develop drugs that can cure or have long-term effect in relieving the symptoms.[4] microRNAs (miRNAs), which are small non-coding RNAs, play significant roles in RNA-silencing and post-transcriptional gene expression regulation. Thus, up-regulation or reduction of a specific miRNA may directly or indirectly regulate T cell imbalance and excessive proliferation of keratinocytes.[2] Studies have identified over 250 miRNAs that exhibit abnormal expression patterns in psoriasis patients, some of which regulate crucial cellular processes such as proliferation,[5,6] differentiation,[7,8] apoptosis,[9] cytokine production[10] and distort T cell subset balance.[2,11,12] Consequently, targeting miRNA has emerged as a promising therapeutic approach for managing psoriasis.[13] There are two approaches in miRNA-based therapy: miRNA inhibition and miRNA replacement. In the former approach, synthetic single-stranded RNAs act as miRNA antagonists (antagomirs) to inhibit the action of endogenous miRNAs. For the replacement approach, miRNA mimics are utilized to mimic the function of endogenous miRNAs, resulting in mRNA degradation/inhibition and inducing a gene silencing effect. For instance, inhibition of miR-210 expression using antagomir-210 reduced Th1 and Th17 differentiation, thereby alleviating symptoms in a mouse model of psoriasis.[14] In another approach, transfection of microRNA-125b (miR-125b) mimic would markedly reduce the HaCaT cell proliferation.[8,15–17] miR-125b has been shown to have multiple targets in

Received: 16 October 2023
Accepted: 29 February 2024
Published: 15 March 2024

Graphical Abstract

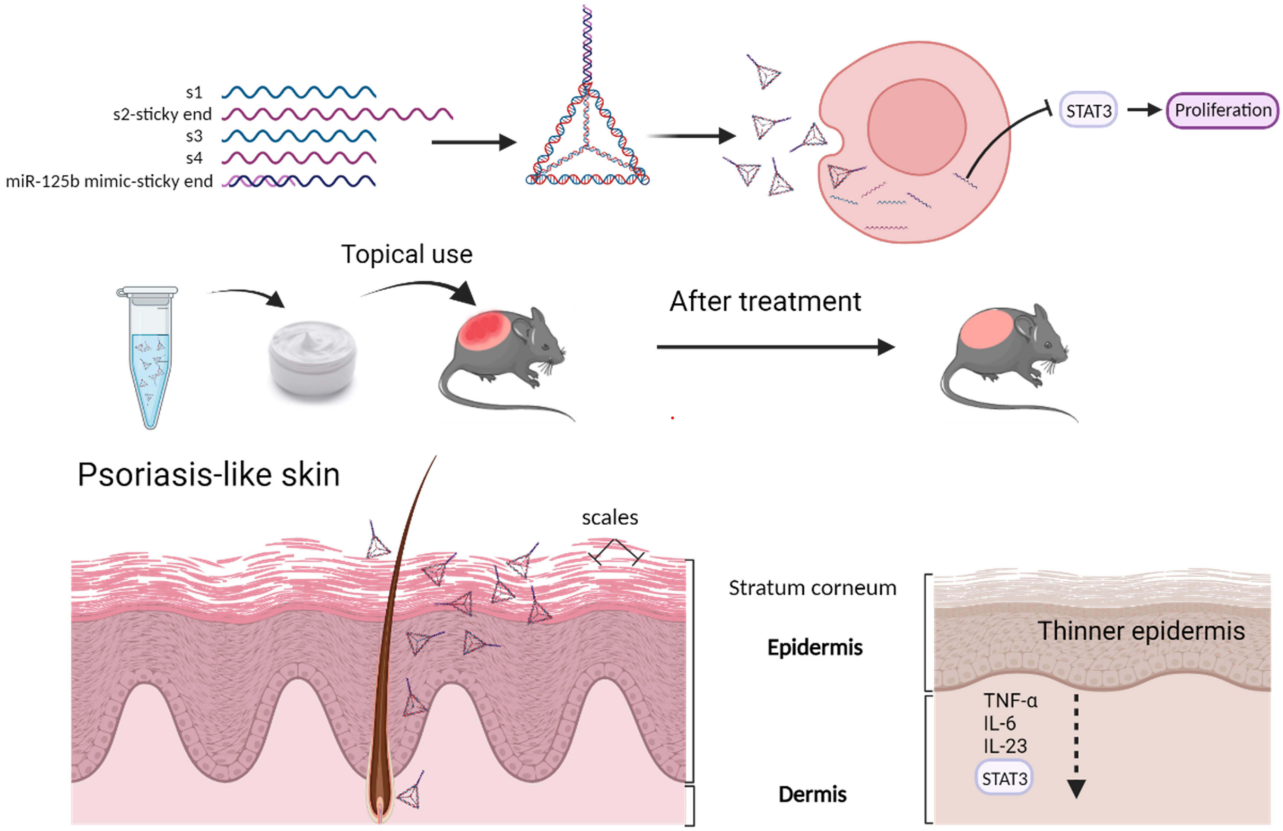

the proliferation of keratinocyte, such as fibroblast growth factor receptor 2 (FGFR2),[6] ubiquitin specific peptidase 2 (USP2),[8] AKT serine/threonine kinase 3 (AKT3)[16] and Bromodomain-containing protein 4 (BRD4).[17] More importantly, Signal Transducer and Activator of Transcription 3 (STAT3) has also been proven to be one of the important targets of miR-125b.[15] STAT3, as an important player in the development of psoriasis, was proved to influence the cell proliferation and contribute to the expansion of T helper cell 17 (Th17).[18,19] Additionally, it has been demonstrated that miR-125b targets TNF-α transcripts at their 3′-UTR.[20] However, regardless of the mechanisms employed, both miRNA antagonists or mimics are susceptible to degradation in vivo.[21] They cannot penetrate through the stratum corneum or enter cells on their own. One potential solution is encapsulation within nanoparticles which can protect them from enzymatic degradation and facilitate cellular uptake.[22]

Framework nucleic acid (FNA) is a three-dimensional DNA nanostructure (nanoparticle) with specific size and shape, capable of efficient internalization via the caveolin-mediated endocytic pathway.[23] FNA has demonstrated successful delivery of doxorubicin through intercalation,[24] positive charged peptide through electrostatic incorporation,[25] and nucleic acids through complementary base pairing.[26] Our team has reported that topically applied tetrahedral FNA nanoparticles could also penetrate through the skin layers and deliver doxorubicin into the subcutaneous tumor.[24] Based on these findings, we propose that FNA holds potential for delivering miRNA drugs into the skin for psoriasis treatment.

As a proof-of-concept, we choose miR-125b mimics as the model miRNA drugs, which is delivered by the tetrahedral FNA. miR-125b is one of the most downregulated miRNAs in psoriasis skin, and its overexpression in primary human keratinocytes would inhibit the cell proliferation and upregulates multiple markers of differentiation.[6] miR-125b mimics is linked at the end of one single strand DNA chain which contains a small sequence offering complementary base pairing sites for connecting. The FNA-miR-125b complex shows higher stability as well as higher cellular internalization

than free miR-125b mimics. In the mouse model, the topically applied FNA-miR-125b could penetrate into the skin and cells, lowering the levels of the downstream target mRNAs like STAT3 and TNF-α. The epidermis thickness and Psoriasis Area and Severity Index (PASI) score are reduced in the psoriasis mice model. Expression of inflammatory cytokines including TNF-α, IL-6, and IL-23 is also reduced.

Methods

Synthesis and Characterization of FNA, FNA-ST and FNA-miR-125b

Four single-stranded DNAs (S1, S2, S3, and S4) were mixed in a Tris-magnesium sulfate buffer (10 mM Tris-HCl and 50 mM $MgCl_2 \cdot 6H_2O$, pH 8.0) at the same molar concentration. The mixture was annealed by heating at 95 °C for 10 min followed by rapid cooling to 4 °C for 20 min to generate FNA. Similarly, FNA-ST was synthesized by replacing S2 with S2-sticky end. FNA-miR-125b was obtained through annealing miR-125b mimic with FNA-ST at room temperature for 2 hours. Cy5-miR-125b mimic was directly ordered from BGI BIO-SOLUTIONS (Hong Kong, China), while Cy5-FNA-miR-125b was prepared totally the same with FNA-miR-125b except for replace miR-125b mimic to Cy5-miR-125b mimic. All nucleic acids used in this study were purchased from BGI BIO-SOLUTIONS, and all the sequences were shown in Table 1.

The hydrodynamic diameters of FNAs were determined using dynamic light scattering (DLS, Malvern, United Kingdom). The quality of FNAs was assessed by agarose gel electrophoresis (or 8% PAGE). The stability of FNAs was evaluated in high-glucose Dulbecco's modified Eagle's medium (DMEM) supplemented with 1% FBS and 10% FBS, respectively, incubated at 37 °C for 1 hour. The control group was treated with DMEM alone. Subsequently, gel electrophoresis was performed to assess the integrity of FNAs.

Cytotoxicity Assays of FNAs

The HaCaT cells were seeded in a 96-well plate at a density of 6000 cells per well. Upon reaching 30–50% confluency, the cells were transfected with miR-125b mimic (100 nM) or FNA-miR-125b (100 nM). After 24, 48, and 72 hours, each well was supplemented with 10 μL of CCK-8 solution (Beyotime, Shanghai, China) diluted in DMEM to a final volume of 100 μL. The plates were then incubated at 37 °C for an additional two hours before measuring the absorbance at a wavelength of 450 nm.

Cell Transfection by FNAs

The HaCaT and NIH/3T3 cells (American Type Culture Collection, ATCC) were cultured in DMEM supplemented with 10% FBS (Thermo Fisher Scientific, USA) and 100 U/mL penicillin-streptomycin at a temperature of 37 °C under a humidified atmosphere containing 5% CO_2. In the transfection experiments, 2×10^5 HaCaT or NIH/3T3 cells were seeded in a six-well plate for 12 hours and then starved in serum-free DMEM for 24 hours. Subsequently, the culture medium was replaced with DMEM containing 1% FBS. Cy5-miR-125b mimic (RiboBio Inc., Guangzhou, China) and Cy5-FNA-miR-125b were added at a final concentration of 100 nM. The positive control group was transfected with Cy5-miR-125b mimic using RNAiMAX (Thermo Fisher Scientific, MA, USA). After incubation for 12 hours, cells were

Table 1 Single Strand DNA and RNA for the Synthesis of Framework Nucleic Acid. (5' to 3')

S1	ATTTATCACCCGCCATAGTAGACGTATCACCAGGCAGTTGAGACGAACATTCCTAAGTCTGAA
S2	ACATGCGAGGGTCCAATACCGACGATTACAGCTTGCTACACGATTCAGACTTAGGAATGTTCG
S2-sticky end	TTGACCTGTGAATTACATGCGAGGGTCCAATACCGACGATTACAGCTTGCTACACGATTCAGACTTAGGAATGTTCG
S3	ACTACTATGGCGGGTGATAAAACGTGTAGCAAGCTGTAATCGACGGGAAGAGCATGCCCATCC
S4	ACGGTATTGGACCCTCGCATGACTCAACTGCCTGGTGATACGAGGATGGGCATGCTCTTCCCG
miR-125b mimic	ucccugagacccuaacuuguga **uucacaggucaa**ucacaaguuagggucucaggga
Cy5-miR-125b mimic	Cy5-ucccugagacccuaacuuguga **uucacaggucaa**ucacaaguuagggucucaggga

collected and analyzed by flow cytometry (BD LSRFortessa; BD Biosciences, USA) to determine transfection efficiency using a sample size of approximately ten thousand cells. Additionally, the fixed cells were stained with Hoechst33342 dye (Invitrogen Corporation, CA, USA) for ten minutes before confocal imaging analysis using TCS SP8 microscope system (Leica Microsystems GmbH; Germany). To identify the target sites of miR-125b mimic treatment on HaCaT cells compared to free miR-125b mimic and FNA-miR-125b treatments as well as positive control group treated with miR-125b mimic using RNAiMAX transfection reagent after forty-eight-hour treatment period.

Preparation and Characterization of miR-125b Mimic and FNA-miR-125b Cream

The cream was obtained by blending an oil-based cream (Emulsifying ointment BP, Mannings, Macau) with 5 μM FNA-ST, 5 μM FNA-miR-125b or 5 μM free miR-125b mimic liquid solution at a weight ratio of 1:1. Blank cream was prepared by water and oil base cream. The ultimate miR-125b mimic loading concentration in the cream was 2.5 nmol/g. The oil-base cream, called Emulsifying ointment BP, was consist of petrolatum, cetearyl alcohol, paraffinum liquidum, sodiumlauryl sulfate. The stability of FNA-ST, FNA-miR-125b and miR-125b mimic in the cream can be tested by agarose gel electrophoresis through diluting the cream by TM buffer.

Establishment of Imiquimod-Induced Psoriasis Mouse Model and Treatment

The animal experiments were conducted in accordance with NIH guidelines and approved by the University of Macau Animal Ethics Committee (Protocol number: UMARE-007-2021). Imiquimod (IMQ) treatment was used to establish the psoriasis-like mouse model.[27] The animal was purchased from FHS Animal Facility at the University of Macau. Specifically, female C57/BL6 mice (6~8-week-old) were divided into six groups (6 mice for each group), and their back skin was treated by hair removal spray foam (Linco Care Ltd, UK) at day 0. On the following day, except the blank control group mice, dorsal skin of each mouse (about 6 cm^2) was applied with 62.5 mg of 5% IMQ (Aldara, 5% imiquimod; Health Care Limited, UK), corresponding to a daily dose of 3.125 mg of the active compound on the skin. After 6 h, except for the blank control group and the IMQ-only treatment, four other groups were treated with 120 mg blank cream, 120 mg FNA cream, 120 mg miR-125b mimic cream or 120 mg FNA-miR-125b cream on the back skin, respectively. The same treatments using IMQ and FNA formulations were repeated on days 2, 3 and 4. On day 5, euthanasia was performed using CO_2 chamber followed by collection of dorsal skin samples for histology and qPCR analysis. Spleen samples were collected for spleen/body weight percentage evaluation.

In another set of experiment, miR-125b mimic cream group and FNA-miR-125b cream group were compared with miR-125b mimic delivered by RNAiMAX and betamethasone (Bet) treatment (4.5mg/kg). The remaining protocols remained unchanged.

In-Vivo Skin Penetration Study

Prior to topical application of the IMQ cream, the back skin of mice was pre-treated with a hair removal spray foam one day in advance. Two groups of mice were administered miR-125b mimic and FNA-miR-125b at a dose of 120 mg cream every 6 hours before IMQ treatment. After 4 days, the mice were sacrificed. In vivo imaging was performed using an In Vivo Imaging System (IVIS, PerkinElmer, USA) both before and after skin removal.

Regarding the in-vivo transdermal efficiency on psoriasis-like mice skin, following 4 consecutive days of IMQ treatment, mice were topically treated with 120 mg of Cy5 miR-125b mimic cream or Cy5-FNA-miR-125b. After 24 hours, the mice were sacrificed, and their back skin was collected and embedded in optimal cutting temperature compound (OCT) for one day. The fixed samples were then sectioned into 10-μm slices and subsequently stained with Hoechst 33,342 before being imaged using confocal laser microscopy (TCS SP8II, Leica, Germany).

Psoriasis Area and Severity Index (PASI) Scores

PASI scores access the severity of psoriasis on the mice. It can be divided to erythema and desquamation independently. Each part was ranging from 0 to 4 with 0 for none, 1 stand for mild condition, 2 for moderate level, 3 means severe level and 4 represent very severe level. The sum of erythema and desquamation scores represent PASI score on the scale of 0 to 8. This assessment was performed for each mouse by two people daily for 5 consecutive days.

Histological Analysis

The skin samples were collected and fixed in 4% paraformaldehyde for one day. Then, the skin samples were under dehydration and embedment by paraffin. The fixed samples were sliced to 4-μm sections and further stained with H&E (hematoxylin and eosin). The imaging was done using light microscope (BDS 200, Aote, China). The thickness of the epidermis was evaluated by Image J.

The Inflammatory Cytokine Measurement in the Mice Skin with Enzyme-Linked Immunosorbent Assay (ELISA)

The fresh mice back skin was individually weighed and placed into separate tubes containing 1 mL of phosphate buffer saline (PBS) with protease inhibitor. The skin tissue was homogenized using the Tissuelyser II Disruption System (Qiagen, CA, USA) at a frequency of 30 per second for 10 minutes, followed by centrifugation at 12,000 RPM at 4 ◦C for 10 minutes. The levels of inflammatory cytokines including TNF-α, IL-23 and IL-6 in the supernatant were quantified using BioLegend ELISA kits (Biolegend, San Diego, CA, USA) according to the manufacturer's instructions.

mRNA and miRNA Quantification by Real-Time PCR (RT-qPCR)

For cell samples, cells were washed twice with PBS and then treated with TRIzol reagent (Takara) to extract RNA. As for skin samples, 50 mg of each sample was cut and placed into a 2 mL centrifuge tube containing 1 mL of TRIzol reagent. All tubes were subsequently subjected to disruption using the Tissuelyser II Disruption System (Qiagen, USA) at a frequency of 30 per second for 10 minutes. The total RNA extraction followed the standard protocol.

For mRNA detection, reverse transcription from RNA to cDNA for mRNA detection was performed using the PrimeScript RT Reagent Kit (Takara, Japan) on the C1000 Touch thermal cycler system instrument (Bio-Rad, UK). For miRNA detection, cDNA synthesis from total RNA was carried out using the Total RNA Reverse Transcription Kit miRNA First Strand cDNA Synthesis Kit Tailing (G3334-25, Servicebio, China). RT-qPCR analysis was conducted on the VIIA7 Real-Time PCR instrument (Applied Biosystems, USA), following the protocol provided by SYBR Premix Ex Taq II kit (Takara, Japan).

The primers used in this study are listed in Table 2 and were purchased from BGI BIO-SOLUTIONS (Hong Kong, China). The primers specific for mmu-miR-125b-5p and U6 were provided by Servicebio (China). The relative levels of target mRNA and miRNA were determined using the comparative Ct method (ΔΔCt). To obtain fold changes as a measure of relative

Table 2 Primer Sequences of Mouse and Genes Examined by *qRT-PCR*

Primer	Base Sequence (5′ to 3′)
Mouse IL-23 (S)	TCCTCCAGCCAGAGGATCACCC
Mouse IL-23 (AS)	AGAGTTGCTGCTCCGTGGGC
Mouse GAPDH (S)	GGGCTCTCTGCTCCTCCCTGT
Mouse GAPDH (AS)	CGGCCAAATCCGTTCACACCG
Mouse TNF-α (S)	GCCCACGTCGTAGCAAACCAC
Mouse TNF-α (AS)	GCAGGGGCTCTTGACGGCAG
Mouse IL-6 (S)	TACCACTTCACAAGTCGGAGGC
Mouse IL-6 (AS)	CTGCAAGTGCATCATCGTTGTTC
Mouse STAT3 (S)	AGCCCATCTGAGTTCAAGACCC
Mouse STAT3 (AS)	GGTTCACCTCATTGTGGAGACC
Human GAPDH (S)	GTCTCCTCTGACTTCAACAGCG
Human GAPDH (AS)	ACCACCCTGTTGCTGTAGCCAA
Human STAT3 (S)	ACAAGUUAGGGUCUCAGGGA
Human STAT3 (AS)	GCCACAATCCGGGCAATCT
Human USP2 (S)	GAGATACGCACCGCGCTTTGTT
Human USP2 (AS)	GGTTGGACTTAGGTCTCAGTGTC
Human AKT3 (S)	CGGAAAGATTGTGTACCGTGATC
Human AKT3 (AS)	CTTCATGGTGGCTGCATCTGTG
Human BRD4 (S)	CGCTATGTCACCTCCTGTTTGC
Human BRD4 (AS)	ACTCTGAGGACGAGAAGCCCTT

quantification, normalization against a reference gene was performed followed by comparison with normalized values. GAPDH served as an internal control gene for mRNA analysis, while U6 was utilized as a control for miRNA analysis.

Statistical Analysis

All the results are described as Mean ± SEM or Mean ± SD, see the notes in each figure for details. GraphPad Prism 8 (GraphPad Software Inc.) was applied for the statistical analysis. The significant difference between multiple groups were performed via repeated measures ANOVA or one-way ANOVA followed by Tukey's honestly significant difference post hoc tests, when $p < 0.05$ was considered as statistically significant.

Result and Discussion

Characterization of FNA and FNA-miR-125b

The synthesis of FNA nanostructures is depicted in Figure 1A, wherein the 5' end of S1 was labeled with Cy5 for imaging purposes. The resulted FNAs were firstly examined in the PAGE gel.[27] As revealed in Figure 1B, it can be observed that the band corresponding to FNA appeared higher than that of a simple mixture comprising S2, S3, and S4. Additionally, the presence of a sticky end on S2 caused a slightly higher migration position for FNA-ST compared to FNA. Notably, upon complexation with miR-125b mimic, the migration rate of FNA further decreased (highest band in the gel). Interestingly, two weak bands were detected in the FNA-miR-125b sample alongside the major one. One of these bands (bottom one) corresponds to FNA-ST, while another might

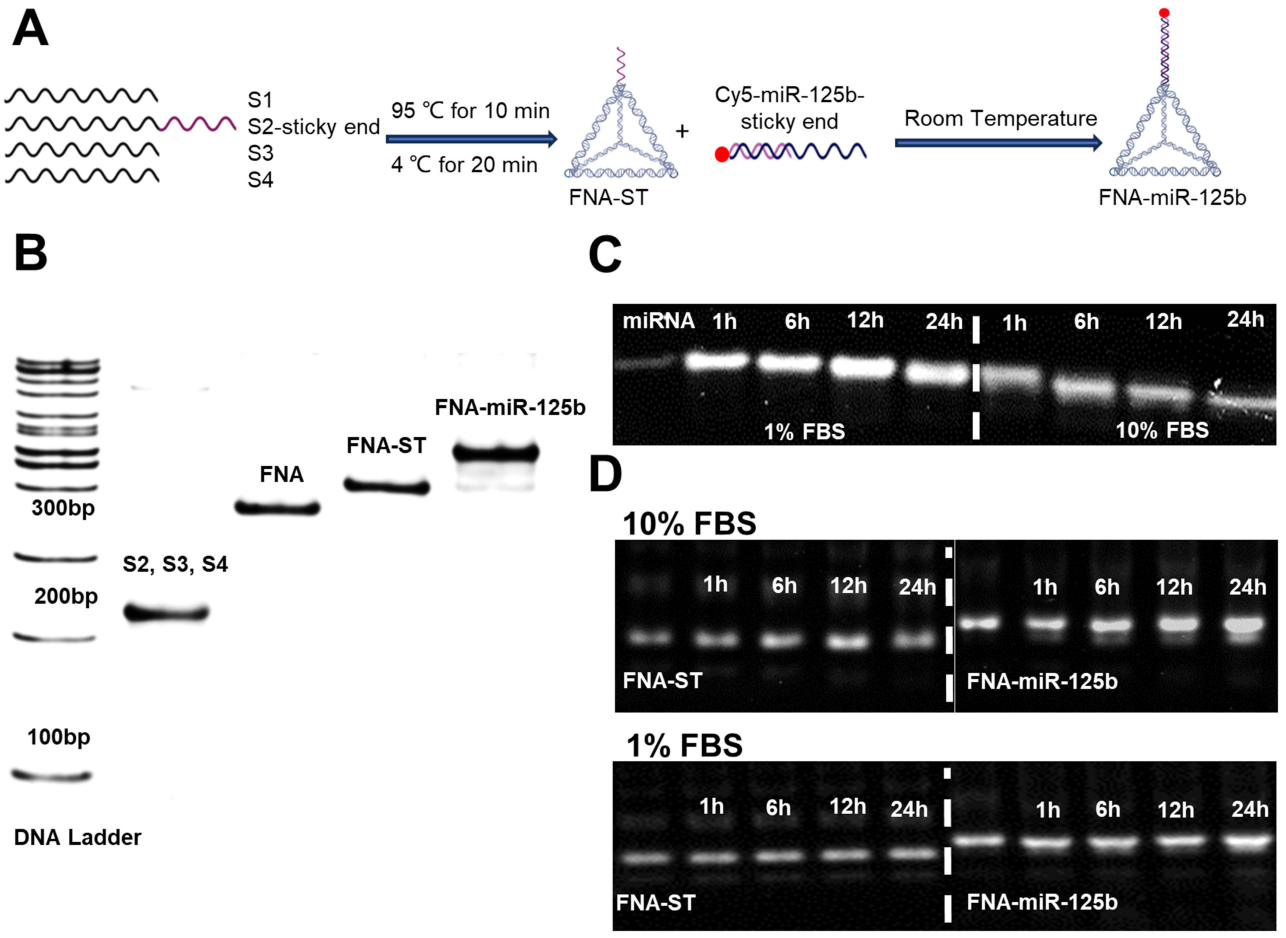

Figure 1 Synthesis and characterization of FNA-miR-125b. (**A**) Illustration of synthesis process; (**B**) Analysis of FNAs through gel electrophoresis (lane 1: DNA Ladder; lane 2: S2, S3 and S4; lane 3: FNA; lane 4: FNA-ST which means FNA with one sticky end on S2; lane 5: FNA-miR-125b); (**C**) Gel electrophoresis of miR-125b mimic treated with 1% FBS and 10% FBS from 1 h to 24 h; (**D**) Gel electrophoresis of FNA-ST and FNA-miR-125b treated with 10% FBS and 1% FBS for 1 h to 24 h.

represent non-complexed FNA-ST+miR-125b (Figure 1B). DLS analysis revealed that the hydrodynamic diameter of FNA-miR-125b was approximately 15 nm (Figure S1). Furthermore, we assessed both consistency and stability by preparing multiple batches of FNA nanostructures. Storage at −20 °C ensured stability for at least one month across all FNAs tested (Figure S2A). Quantification based on relevant band intensities also indicated consistent yields among different batches synthesized (Figure S2B).

The stability of miR-125b mimic and FNA-miR-125b in DMEM with 1% FBS and 10% FBS was subsequently assessed. As depicted in Figure 1C, the degradation of miR-125b mimic was observed in the presence of FBS, with a higher concentration leading to a faster degradation rate. In contrast, both FNA-ST and FNA-miR-125b exhibited remarkable stability under both 1% and 10% FBS conditions (Figure 1D).

Cellular Uptake of FNA-miR-125b and Its Function Analysis

Since the FNAs exhibited minimal degradation in a buffer containing 1% FBS over a period of 12 hours (Figure 1D), HaCaT and NIH/3T3 cells were treated with either miR-125b mimic alone, FNA-miR-125b, or miR-125b mimic+RNAiMAX (positive control) in a buffer containing 1% FBS system for 12 hours. Flow cytometry analysis revealed significantly higher cellular uptake of both FNA-miR-125b and the positive control compared to miR-125b mimic alone in both HaCaT (Figures 2A and S3A) and NIH/3T3 cells (Figures 2B and S3B). However, RNAiMAX outperformed FNA as demonstrated in Figure S3A and S3B. The successful internalization of FNA-miR-125b was further confirmed through confocal imaging (Figure 2D).

miR-125b has been reported to inhibit hyperproliferation of keratinocytes. Therefore, we monitored the proliferation of HaCaT cells (a keratinocyte cell line) after treatment with miR-125b mimic alone, FNA-miR-125b or miR-125b mimic +RNAiMAX (Figure 2C). While the positive control (miR-125b mimic + RNAiMAX) showed the strongest inhibition of HaCaT proliferation, FNA-miR-125b also significantly suppressed cell proliferation. This result is consistent with the cell uptake results (Figure 2A and B), where improved uptake of miR-125b would generate higher inhibition of HaCaT proliferation. Additionally, to exclude any additional interference, a negative control miRNA mimic transfected by RNAiMAX was applied. The negative control group (miR-NC + RNAiMAX) did not show an obvious influence on HaCaT cell proliferation (Figure S4A and S4B). Furthermore, miR-125b can inhibit the HaCaT cell proliferation under the treatment of imiquimod (IMQ) (Figure S4C).

In addition to inhibiting proliferation, we further investigated the impact of altered cellular concentration of miR-125b on downstream target mRNAs (USP2, BRD4, AKT3, and STAT3), which have been previously identified as targets in HaCaT cells by other researchers. HaCaT cells were treated with miR-125b mimic, miR-125b mimic+RNAiMAX, and FNA-miR-125b at the same concentration (100 nM) for 48 h. As depicted in Figure 2E, both the miR-125b mimic +RNAiMAX group and FNA-miR-125b significantly downregulated STAT3 expression compared to the naked miR-125b mimic group. Furthermore, we confirmed that FNA-miR-125b can also downregulate other target mRNAs such as USP2, BRD4, and AKT3 (Figure S3C).

Skin Penetration Capability of FNA-miR-125b

To facilitate administration, we homogenized the aqueous sample solution with an oil-based cream to obtain a white cream formulation (Figure S5A). Furthermore, we investigated and determined that the optimal weight ratio of oil-based cream to aqueous solution is 1:1. Excessive aqueous phase resulted in residual solution that could not be fully incorporated into the cream matrix (Figure S5B). Subsequently, stability evaluation of FNA-ST cream, FNA-miR-125b cream, and miR-125b mimic cream was conducted by storing the samples at 4 °C (Figure S5C), demonstrating stable formulation integrity for a period ranging from 3 to 7 days. We assessed the cutaneous permeability of FNA-miR-125b using in vivo models. Topical application of either Cy5-FNA-miR-125b or Cy5-miR-125b cream was performed on a psoriasis mouse model. After 24 hours, enhanced fluorescence was observed in mice treated with Cy5-FNA-miR-125b, whereas no significant fluorescence signal was detected in those treated with Cy5-miR-125b (Figure 3A). Histological analysis demonstrated that FNA-miR-125b penetrated the skin through both hair follicles and the stratum corneum (Figure 3B). Notably, FNA-miR-125b exhibited deeper penetration into the skin via hair follicles, while its distribution within the epidermis layer

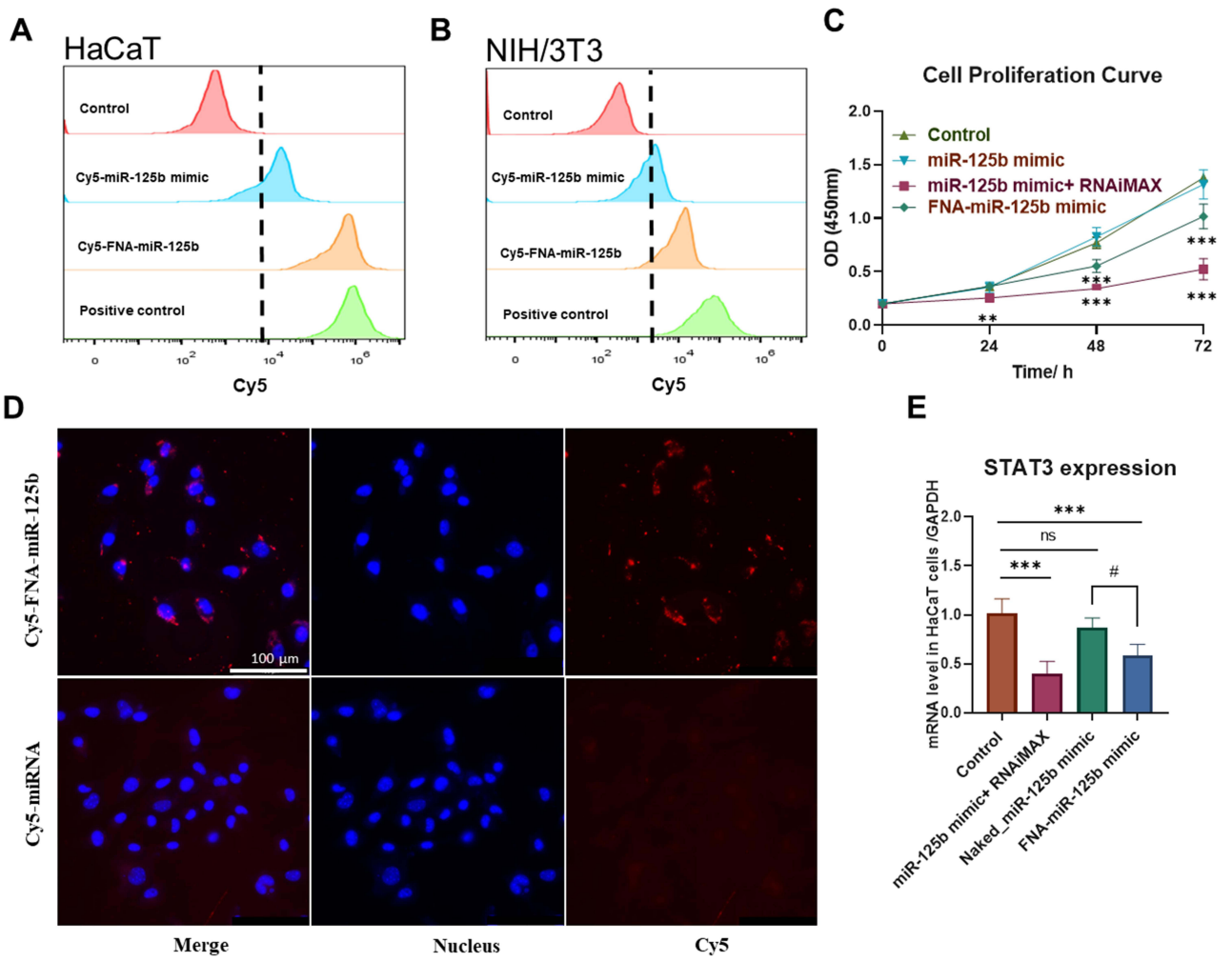

Figure 2 Cellular uptake and the mRNA levels of targeting genes of FNA-miR-125b. (**A**) Flow cytometry analysis of HaCaT cells labeled with miR-125b mimic alone, FNA-miR-125b or miR-125b mimic+RNAiMAX (positive control); (**B**) Flow cytometry analysis of NIH/3T3 cells labeled with miR-125b mimic alone, FNA-miR-125b or miR-125b mimic+RNAiMAX (positive control); (**C**) The proliferation curve of HaCaT cells after the treatment of miR-125b mimic, FNA-miR-125b or miR-125b mimic+RNAiMAX at 24 h, 48 h and 72 h; (**D**) The imaging of cellular uptake of Cy5-FNA-miR-125b and Cy5-miR-125b mimic in HaCaT cell by a DMI8 laser microscope (nucleus: blue Cy5: red). Scale bars are 100 μm. (**E**) The quantification of STAT3 expression level after cell transfection with miR-125b mimic, FNA-miR-125b or miR-125b mimic+RNAiMAX at 48 h. In all the images, data is presented as mean ± SD (n≥3), $^{**}p < 0.01$, $^{***}p < 0.001$, $^{\#}p < 0.05$, *ns* refers "not significant" and $p > 0.05$.

appeared more homogeneous. Conversely, negligible fluorescence signal was observed in skin tissues from mice treated with Cy5-miR-125b.

The Topical Treatment of FNA-miR-125b Cream for Psoriasis Mice Model

The psoriasis-like symptom was induced on the dorsal skin of mice through IMQ treatment (Figure 4A). The symptoms of skin desquamation and erythema began to manifest from day 2 and intensified with prolonged IMQ treatment (Figure 4E). Compared to the blank control group (healthy mice), both the IMQ group (psoriasis mice without any treatment) and the blank cream group (psoriasis mice treated with blank cream) exhibited more pronounced psoriasis symptoms, such as white scales, erythema, and increased skin thickness (Figure 4B and E). However, these symptoms were alleviated when the mice were treated with FNA-ST, miR-125b mimic, or FNA-miR-125b.

Histological examination and analysis of mouse skin after a 4-day treatment revealed that normal mouse epidermis consisted of a single layer of basal cells, while psoriatic mouse skin displayed multilayered basal cells (Figure 4C and D). Application of both blank cream and FNA-ST cream did not alter this hyperproliferation phenomenon. Conversely,

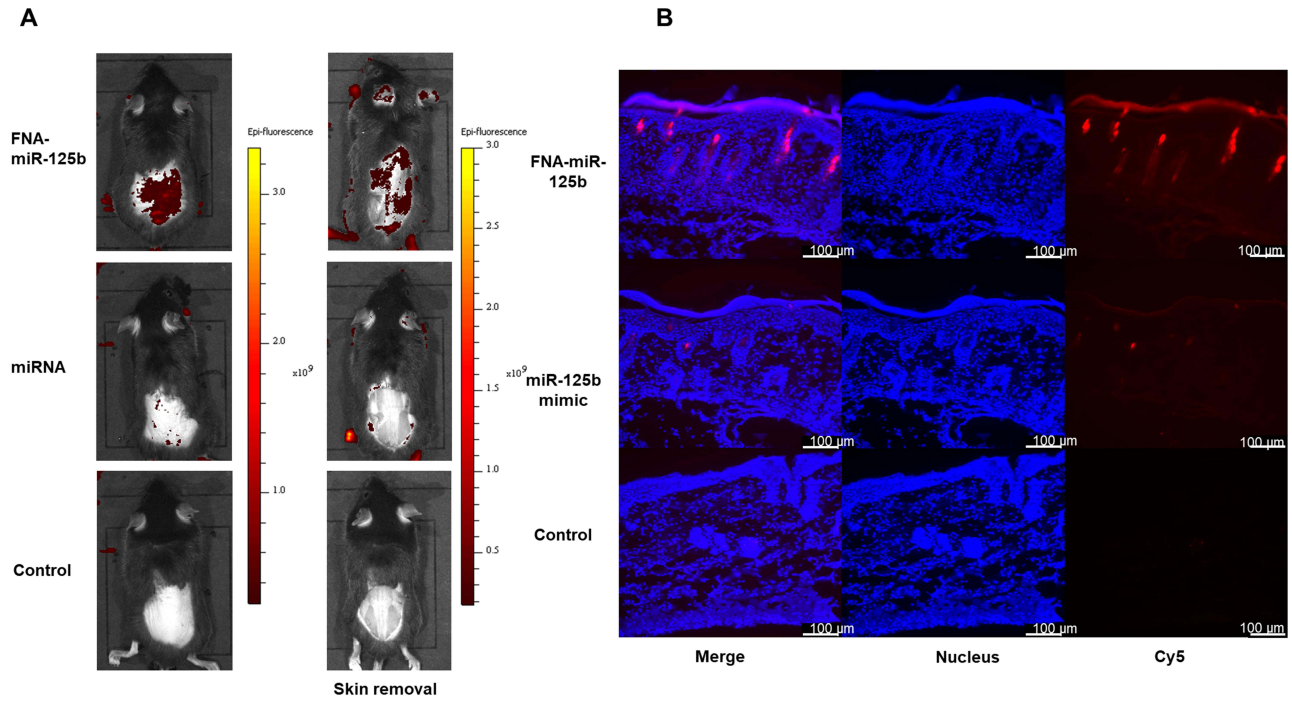

Figure 3 Skin penetration capability of FNA-miR-125b in the mouse back skin. (**A**) IVIS in vivo imaging; (**B**) Histology analysis of skin section post the treatment of FNA-miR-125b and miR-125b mimic (nucleus: blue Cy5: red).

treatment with miR-125b mimic and particularly FNA-miR-125b cream reduced epidermal thickness. As quantified in Figure 4E, the average thickness of the epidermis in the FNA-miR-125b cream-treated group was approximately 20 μm less than that observed in the untreated psoriasis group.

Inflammatory Cytokines Level Measure

Besides analyzing psoriatic symptoms, we conducted a study on the inflammatory cytokines (TNF-α, IL-6, and IL-23) associated with the therapeutic index and severity of psoriasis.[27,28] Figure 5A and B illustrate the correlated mRNA and protein levels of these cytokines, respectively. The expression of all key cytokines was increased following IMQ treatment. However, when mice were treated with FNA cream, both mRNA and protein levels of TNF-α, IL-6, and IL-23 exhibited a significant reduction compared to the IMQ group ($p < 0.05$). Importantly, blank cream treatment had no impact, while FNA demonstrated a pronounced anti-inflammatory effect consistent with previous reports.[29,30] The most favorable outcome was observed in the FNA-miR-125b cream group due to the inherent anti-inflammatory properties of FNA itself as well as its potential inhibition of inflammation through miR-125b mimic;[20,31,32] moreover, it is worth mentioning that enhanced penetration of miR-125b mimic played a crucial role. In conjunction with the penetration results depicted in Figure 3, it is evident that the therapeutic efficacy of miR-125b is intricately associated with its accumulation within the skin. Despite FNA-miR-125b being predominantly distributed in the epidermis and hair follicles, it adequately modulates the inflammatory milieu of the skin's epidermal layer. Our previous investigations have also substantiated that targeting epidermal keratinocytes as a therapeutic strategy can ameliorate psoriasis severity.[33]

Comparison of FNA Formulation with the Clinical Standards

In the aforementioned experiments, we have substantiated the efficacy of FNA-miR-125b cream in alleviating psoriasis symptoms. Subsequently, we conducted additional animal experiments to compare the effects of FNA-miR-125b with miR-125b+RNAiMAX and betamethasone cream, which is commonly used in clinical practice (Figure 6A). Consistent with the findings presented in Figure 4, psoriasis symptoms were induced using IMQ treatment (Figure 6B). Remarkably,

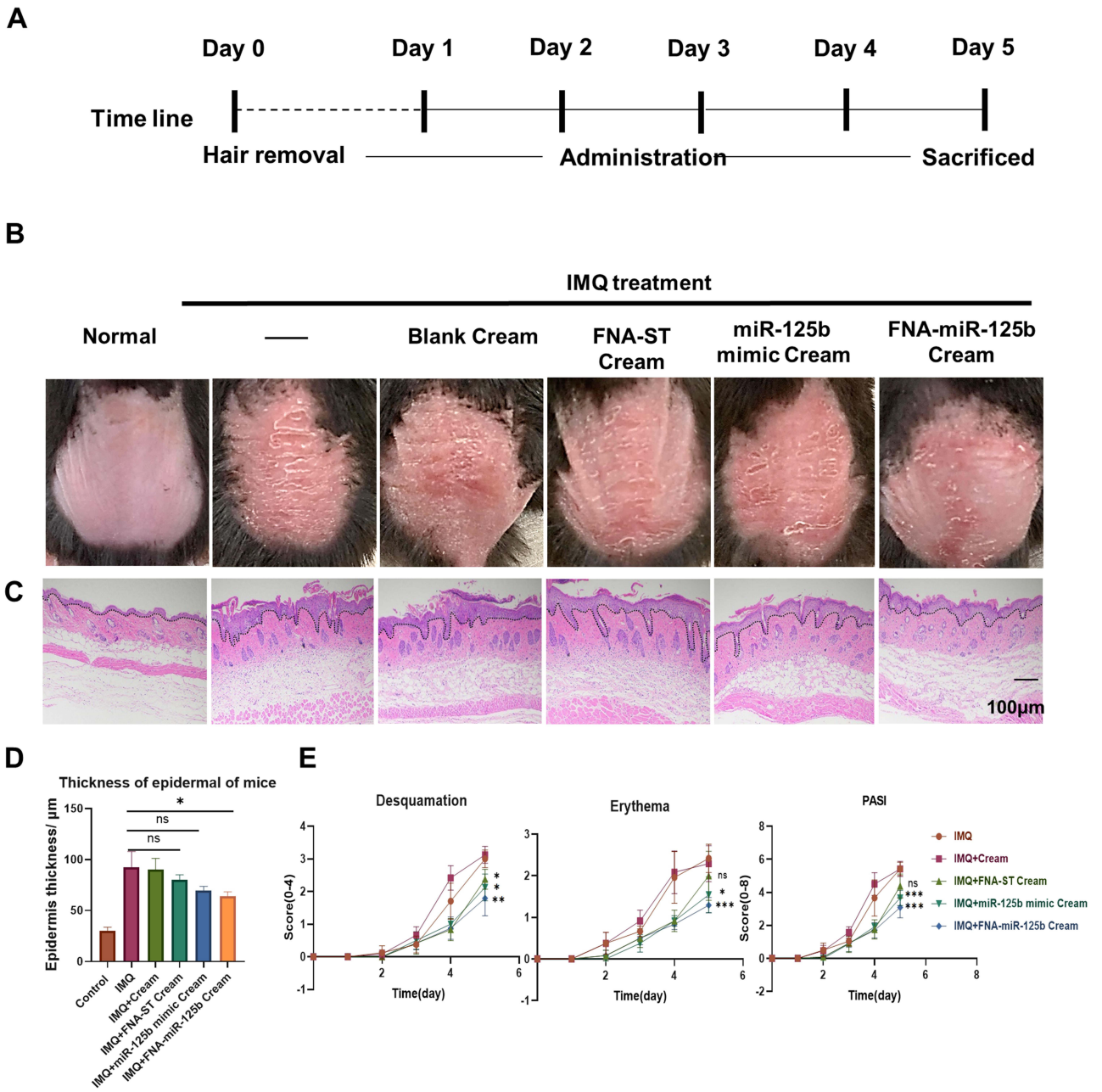

Figure 4 Psoriatic symptom of the mice dorsal skin under treatment. (**A**) The timeline of the animal experiment; (**B, C**) The images of the back skin and H&E sections after 4-day treatment; (**D**) The quantification of epidermis thickness of mouse skin in different treatment groups; (**E**) The PASI scores, including erythema, desquamation and PASI total score of back skin recorded for 5 days. Data are presented as mean ± SD (n = 6), *$p < 0.05$, **$p < 0.01$, ***$p < 0.001$, *ns* refers "not significant" and $p > 0.05$.

all groups treated with miR-125b, and betamethasone exhibited significant relief compared to the group subjected solely to IMQ treatment (Figure 6B).

Regarding the spleen/body weight ratio, the positive drug group treated with betamethasone cream exhibited a significantly greater reduction in spleen weight ratio ($p < 0.001$), while the FNA-miR-125b group showed the most significant reduction otherwise ($p < 0.01$) (Figure 6C). In comparison to the IMQ treatment group, both the FNA-miR-125b and miR-125b with RNAiMAX groups demonstrated a significant increase in miR-125b levels ($p < 0.05$) as depicted in Figure 6D. To investigate miR-125b targets in this mouse model, considering interspecies variation between mice and humans, we selected TNF-α and STAT3 as two validated target mRNAs for assessing mRNA levels (Figure 6E). The free miR-125b mimic cream group displayed a significant decrease in TNF-α expression ($p < 0.001$) and STAT3 expression ($p < 0.01$) compared to IMQ treatment alone. Notably, STAT3 expression was significantly reduced in the miR-

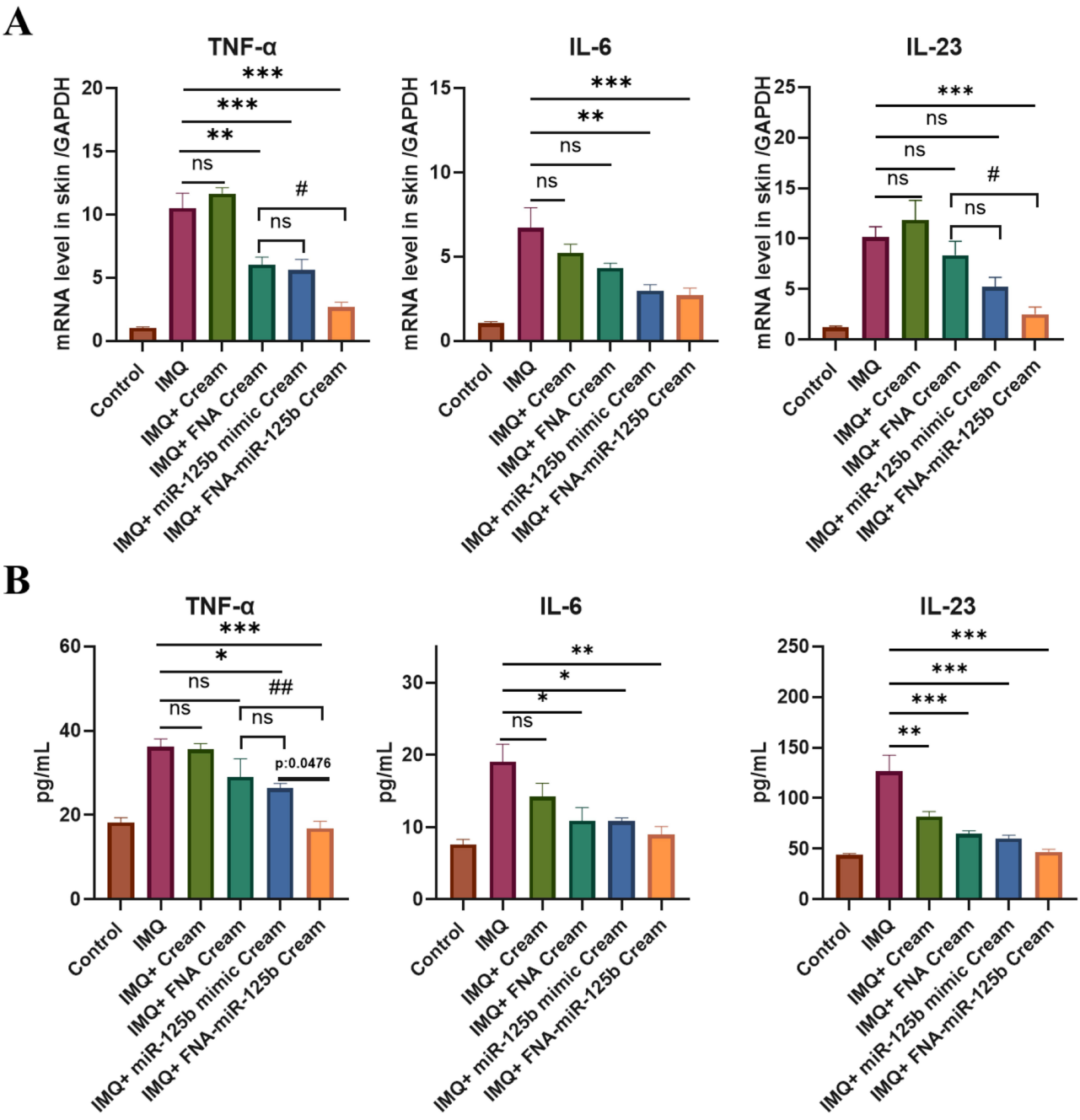

Figure 5 The expression of inflammatory cytokines mRNA in the psoriasis mouse skin after different treatment. (**A**) The mRNA levels of TNF-α, IL-6, and IL-23 in skin lesion; (**B**) The protein level of TNF-α, IL-6, and IL-23 in skin lesion. *$p < 0.05$, **$p < 0.01$, ***$p < 0.001$, $^{\#}p < 0.05$, $^{\#\#}p < 0.01$, not significant $p > 0.05$. Each value represents the mean and SEM ($n = 6$).

125b_RNAiMAX group ($p < 0.05$). The relatively higher level of TNF-α observed in the miR-125b_RNAiMAX group may be attributed to two aspects. Firstly, lower penetration of the cationic lipid-miRNA complex. Since the formulation of miR-125b_RNAiMAX is a simple complex instead of nanoparticle, it might not suitable for topical delivery. Additionally, cationic lipid addition in RNAiMAX might trigger more serious symptom, since previous studies have shown that cationic lipids can trigger immune responses and release inflammatory cytokines.[34–36] Overall, the use of cationic lipid in skin disorder required careful design to ensure the safety issue. FNA-miR-125b performed the best, significantly decreased TNF-α ($p < 0.001$), and STAT3 ($p < 0.01$) compared to IMQ group.

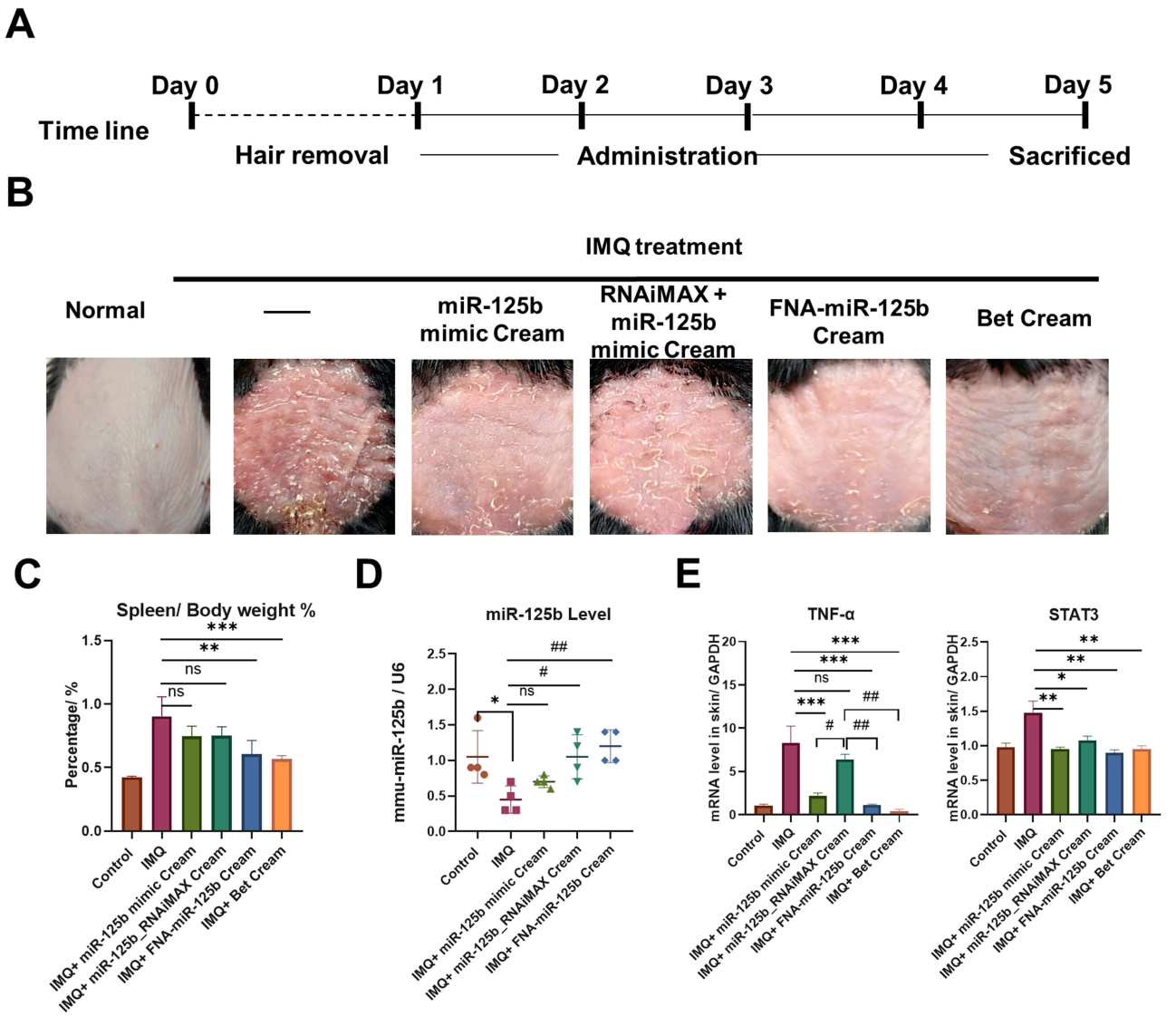

Figure 6 Psoriatic symptom of the mice dorsal skin under treatment with betamethasone as positive control. (**A**) The timeline of the animal experiment; (**B**) The images of the back skin after 4 days' administration; (**C**) The spleen/body (%, *w*/*w*) was calculated on Day 5. $^{**}p < 0.01$, $^{***}p < 0.001$, not significant $p > 0.05$; (**D**) mmu-miR-125b level in skin lesion. $^{*}p < 0.05$ compared with control group. $^{\#}p < 0.05$, $^{\#\#}p < 0.01$, not significant, $p > 0.05$, compared with IMQ group; (**E**) mRNA level of TNF-α and STAT3 in skin lesion. Data are presented as mean ± SEM (n = 4). $^{*}p < 0.05$, $^{**}p < 0.01$, $^{***}p < 0.001$, $^{\#}p < 0.05$, $^{\#\#}p < 0.01$, not significant $p > 0.05$.

Conclusions

This study demonstrates the usage of FNA nanostructure as the topical miRNA delivery system in psoriasis treatment, where miR-125b mimic was chosen as a model drug. Compared with the naked miR-125b mimic, FNA-miR-125b showed better inhibition of the proliferation of HaCaT cells, higher knock down efficiency for downstream target mRNAs like STAT3 and TNF-α and much better skin penetration efficiency. Finally, in the IMQ-induced psoriasis mouse model, FNA-miR-125b provided the best treatment outcome, like the least proliferation of epidermal and the lowest levels of key inflammatory cytokines.

Acknowledgment

This work was supported by research grants from the Macau Science and Technology Development Fund (0086/2021/A2) and Shenzhen Fundamental Research Program (EF022/ICMS-ZY/2022/SZSTIC). We thank the members of the FHS Animal Facility at the University of Macau for their experimental and technical support. C.X. also appreciates the

support of General Research Fund (GRF) grant from the Research Grants Council (RGC) of the Hong Kong Special Administrative Region, China (CityU 11202021).

Disclosure

The authors declare no conflicts of interest in this work.

References

1. Greb JE, Goldminz AM, Elder JT, et al. Psoriasis. *Nat Rev Dis Primers*. 2016;2(1):16082. doi:10.1038/nrdp.2016.82
2. Xiuli Y, Honglin W. miRNAs Flowing Up and Down: the Concerto of Psoriasis. *Front Med*. 2021;8. doi:10.3389/fmed.2021.646796
3. Jiang X, Huang S, Cai W, et al. Glutamine-Based Metabolism Normalization and Oxidative Stress Alleviation by Self-Assembled Bilirubin/V9302 Nanoparticles for Psoriasis Treatment. *Adv Healthcare Mater*. 2023;12(13):2203397. doi:10.1002/adhm.202203397
4. Jiang X, Yao Q, Xia X, et al. Self-assembled nanoparticles with bilirubin/JPH203 alleviate imiquimod-induced psoriasis by reducing oxidative stress and suppressing Th17 expansion. *Chem Eng J*. 2022;431:133956. doi:10.1016/j.cej.2021.133956
5. Shen H, Tian Y, Yao X, Liu W, Zhang Y, Yang Z. MiR-99a inhibits keratinocyte proliferation by targeting Frizzled-5 (FZD5) / FZD8 through β-catenin signaling in psoriasis. *Die Pharmazie*. 2017;72(8):461–467. doi:10.1691/ph.2017.7018
6. Xu N, Brodin P, Wei T, et al. MiR-125b, a MicroRNA Downregulated in Psoriasis, Modulates Keratinocyte Proliferation by Targeting FGFR2. *J Invest Dermatol*. 2011;131(7):1521–1529. doi:10.1038/jid.2011.55
7. Lerman G, Avivi C, Mardoukh C, et al. MiRNA Expression in Psoriatic Skin: reciprocal Regulation of hsa-miR-99a and IGF-1R. *PLoS One*. 2011;6(6):e20916. doi:10.1371/journal.pone.0020916
8. Wei T, Folkersen L, Biskup E, et al. Ubiquitin-specific peptidase 2 as a potential link between microRNA-125b and psoriasis. *Br J Dermatol*. 2017;176(3):723–731. doi:10.1111/bjd.14916
9. Jia H-Y, Zhang K, W-J L, G-W X, Zhang J-F, Tang Z-L. LncRNA MEG3 influences the proliferation and apoptosis of psoriasis epidermal cells by targeting miR-21/caspase-8. *BMC Mol Cell Biol*. 2019;20(1):46. doi:10.1186/s12860-019-0229-9
10. Srivastava A, Nikamo P, Lohcharoenkal W, et al. MicroRNA-146a suppresses IL-17–mediated skin inflammation and is genetically associated with psoriasis. *J Allergy Clin Immunol*. 2017;139(2):550–561. doi:10.1016/j.jaci.2016.07.025
11. Deng Y, Chang C, Lu Q. The Inflammatory Response in Psoriasis: a Comprehensive Review. *Clin Rev Allergy Immunol*. 2016;50(3):377–389. doi:10.1007/s12016-016-8535-x
12. Feng H, Wu R, Zhang S, et al. Topical administration of nanocarrier miRNA-210 antisense ameliorates imiquimod-induced psoriasis-like dermatitis in mice. *J Dermatol*. 2020;47(2):147–154. doi:10.1111/1346-8138.15149
13. Pradyuth S, Rapalli VK, Gorantla S, Waghule T, Dubey SK, Singhvi G. Insightful exploring of microRNAs in psoriasis and its targeted topical delivery. *Dermatologic Therapy*. 2020;33(6):e14221. doi:10.1111/dth.14221
14. Wu R, Zeng J, Yuan J, et al. MicroRNA-210 overexpression promotes psoriasis-like inflammation by inducing Th1 and Th17 cell differentiation. *J Clin Invest*. 2018;128(6):2551–2568. doi:10.1172/JCI97426
15. Yang Z, Chen Z, Wang C, Huang P, Luo M, Zhou R. STAT3/SH3PXD2A-AS1/miR-125b/STAT3 positive feedback loop affects psoriasis pathogenesis via regulating human keratinocyte proliferation. *Cytokine*. 2021;144:155535. doi:10.1016/j.cyto.2021.155535
16. Zheng Y, Cai B, Li X, Li D, Yin G. MiR-125b-5p and miR-181b-5p inhibit keratinocyte proliferation in skin by targeting Akt3. *Eur J Pharmacol*. 2019;862:172659. doi:10.1016/j.ejphar.2019.172659
17. Pan M, Huang Y, Zhu X, Lin X, Luo D. miR-125b-mediated regulation of cell proliferation through the Jagged-1/Notch signaling pathway by inhibiting BRD4 expression in psoriasis. *Mol Med Rep*. 2019;19(6):5227–5236. doi:10.3892/mmr.2019.10187
18. Chen R, Zhai -Y-Y, Sun L, et al. Alantolactone-loaded chitosan/hyaluronic acid nanoparticles suppress psoriasis by deactivating STAT3 pathway and restricting immune cell recruitment. *Asian J Pharm Sci*. 2022;17(2):268–283. doi:10.1016/j.ajps.2022.02.003
19. Yan K, Zhang F, Ren J, Huang Q, Yawalkar N, Han L. MicroRNA-125a-5p regulates the effect of Tregs on Th1 and Th17 through targeting ETS-1/STAT3 in psoriasis. *J Transl Med*. 2023;21(1):678. doi:10.1186/s12967-023-04427-6
20. Tili E, Michaille -J-J, Cimino A, et al. Modulation of miR-155 and miR-125b levels following lipopolysaccharide/TNF-α stimulation and their possible roles in regulating the response to endotoxin shock. *J Immunol*. 2007;179(8):5082–5089.
21. Roberts TC, Langer R, Wood MJA. Advances in oligonucleotide drug delivery. *Nat Rev Drug Discov*. 2020;19(10):673–694. doi:10.1038/s41573-020-0075-7
22. Lee SWL, Paoletti C, Campisi M, et al. MicroRNA delivery through nanoparticles. *J Control Release*. 2019;313:80–95. doi:10.1016/j.jconrel.2019.10.007
23. Ding H, Li J, Chen N, et al. DNA Nanostructure-Programmed Like-Charge Attraction at the Cell-Membrane Interface. *ACS Cent. Sci*. 2018;4(10):1344–1351. doi:10.1021/acscentsci.8b00383
24. Wiraja C, Zhu Y, Lio DCS, et al. Framework nucleic acids as programmable carrier for transdermal drug delivery. *Nat Commun*. 2019;10(1):1147. doi:10.1038/s41467-019-09029-9
25. Liu Y, Sun Y, Li S, et al. Tetrahedral Framework Nucleic Acids Deliver Antimicrobial Peptides with Improved Effects and Less Susceptibility to Bacterial Degradation. *Nano Lett*. 2020;20(5):3602–3610. doi:10.1021/acs.nanolett.0c00529
26. Xiao D, Li Y, Tian T, et al. Tetrahedral Framework Nucleic Acids Loaded with Aptamer AS1411 for siRNA Delivery and Gene Silencing in Malignant Melanoma. *ACS Appl Mater Interfaces*. 2021;13(5):6109–6118. doi:10.1021/acsami.0c23005
27. Xi L, Lin Z, Qiu F, et al. Enhanced uptake and anti-maturation effect of celastrol-loaded mannosylated liposomes on dendritic cells for psoriasis treatment. *Acta Pharmaceutica Sinica B*. 2022;12(1):339–352. doi:10.1016/j.apsb.2021.07.019
28. Sun L, Liu Z, Wang L, et al. Enhanced topical penetration, system exposure and anti-psoriasis activity of two particle-sized, curcumin-loaded PLGA nanoparticles in hydrogel. *J Control Release*. 2017;254:44–54. doi:10.1016/j.jconrel.2017.03.385
29. Yang X, Zhang F, Du Y, et al. Effect of tetrahedral DNA nanostructures on LPS-induced neuroinflammation in mice. *Chin. Chem. Lett*. 2022;33(4):1901–1906. doi:10.1016/j.cclet.2021.10.029

30. Zhang Q, Lin S, Shi S, et al. Anti-inflammatory and Antioxidative Effects of Tetrahedral DNA Nanostructures via the Modulation of Macrophage Responses. *ACS Appl Mater Interfaces*. 2018;10(4):3421–3430. doi:10.1021/acsami.7b17928
31. Guo Z, Gu Y, Wang C, et al. Enforced expression of miR-125b attenuates LPS-induced acute lung injury. *Immunol Lett*. 2014;162(1, Part A):18–26. doi:10.1016/j.imlet.2014.06.008
32. Chen X-M, Gao K-X, Wu X-D, et al. Chinese Herbal Formula Huayu-Qiangshen-Tongbi Decoction Attenuates Rheumatoid Arthritis through Upregulating miR-125b to Suppress NF-κB-Induced Inflammation by Targeting CK2. *J Immunol Res*. 2022;2022:2836128. doi:10.1155/2022/2836128
33. Qiu F, Xi L, Chen S, Zhao Y, Wang Z, Zheng Y. Celastrol Niosome Hydrogel Has Anti-Inflammatory Effect on Skin Keratinocytes and Circulation without Systemic Drug Exposure in Psoriasis Mice. *Int j Nanomed*. 2021;16:6171–6182. doi:10.2147/IJN.S323208
34. Jörgensen AM, Wibel R, Bernkop-Schnürch A. Biodegradable Cationic and Ionizable Cationic Lipids: a Roadmap for Safer Pharmaceutical Excipients. *Small*. 2023;19(17):2206968. doi:10.1002/smll.202206968
35. Zhang H, Han X, Alameh M-G, et al. Rational design of anti-inflammatory lipid nanoparticles for mRNA delivery. *J Biomed Mater Res Part A*. 2022;110(5):1101–1108. doi:10.1002/jbm.a.37356
36. Parhiz H, Brenner JS, Patel PN, et al. Added to pre-existing inflammation, mRNA-lipid nanoparticles induce inflammation exacerbation (IE). *J Control Release*. 2022;344:50–61. doi:10.1016/j.jconrel.2021.12.027